

Dear Author

Here are the proofs of your article.

- You can submit your corrections **online**, via **e-mail** or by **fax**.
- For **online** submission please insert your corrections in the online correction form. Always indicate the line number to which the correction refers.
- You can also insert your corrections in the proof PDF and **email** the annotated PDF.
- For **fax** submission, please ensure that your corrections are clearly legible. Use a fine black pen and write the correction in the margin, not too close to the edge of the page.
- Remember to note the **journal title**, **article number**, and **your name** when sending your response via e-mail or fax.
- **Check** the metadata sheet to make sure that the header information, especially author names and the corresponding affiliations are correctly shown.
- **Check** the questions that may have arisen during copy editing and insert your answers/corrections.
- **Check** that the text is complete and that all figures, tables and their legends are included. Also check the accuracy of special characters, equations, and electronic supplementary material if applicable. If necessary refer to the *Edited manuscript*.
- The publication of inaccurate data such as dosages and units can have serious consequences. Please take particular care that all such details are correct.
- Please **do not** make changes that involve only matters of style. We have generally introduced forms that follow the journal's style.
- Substantial changes in content, e.g., new results, corrected values, title and authorship are not allowed without the approval of the responsible editor. In such a case, please contact the Editorial Office and return his/her consent together with the proof.
- If we do not receive your corrections **within 48 hours**, we will send you a reminder.
- Your article will be published **Online First** approximately one week after receipt of your corrected proofs. This is the **official first publication** citable with the DOI. **Further changes are, therefore, not possible.**
- The **printed version** will follow in a forthcoming issue.

Please note

After online publication, subscribers (personal/institutional) to this journal will have access to the complete article via the DOI using the URL:

<http://dx.doi.org/10.1007/s00170-016-9960-y>

If you would like to know when your article has been published online, take advantage of our free alert service. For registration and further information, go to:

<http://www.link.springer.com>.

Due to the electronic nature of the procedure, the manuscript and the original figures will only be returned to you on special request. When you return your corrections, please inform us, if you would like to have these documents returned.

Metadata of the article that will be visualized in OnlineFirst

Please note: Images will appear in color online but will be printed in black and white.

1	Article Title	Sintering of 17-4PH stainless steel powder assisted by microwave and the gradient of mechanical properties in the sintered body	
2	Article Sub- Title		
3	Article Copyright - Year	Springer-Verlag London 2017 (This will be the copyright line in the final PDF)	
4	Journal Name	The International Journal of Advanced Manufacturing Technology	
5		Family Name	Barriere
6		Particle	
7		Given Name	T.
8		Suffix	
9	Corresponding Author	Organization	Femto-ST Institute
10		Division	UBFC, Department of Applied Mechanics
11		Address	Besançon, 24 Rue de l'Epitaphe, Besançon 25030
12		e-mail	thierry.barriere@univ-fcomte.fr
13		Family Name	Shi
14		Particle	
15		Given Name	J.
16		Suffix	
17		Organization	Southwest University of Science and Technology
18		Division	School of Civil Engineering and Architecture
19		Address	Mianyang 621010
20	Author	Organization	Southwest Jiaotong University
21		Division	School of Mechanics and Engineering
22		Address	Chengdu 610031
23		Organization	Femto-ST Institute
24		Division	UBFC, Department of Applied Mechanics
25		Address	Besançon, 24 Rue de l'Epitaphe, Besançon 25030
26		e-mail	
27	Author	Family Name	Cheng
28		Particle	

29		Given Name	Z.
30		Suffix	
31		Organization	Southwest Jiaotong University
32		Division	School of Mechanics and Engineering
33		Address	Chengdu 610031
34		e-mail	
<hr/>			
35		Family Name	Gelin
36		Particle	
37		Given Name	J.C.
38		Suffix	
39	Author	Organization	Femto-ST Institute
40		Division	UBFC, Department of Applied Mechanics
41		Address	Besançon, 24 Rue de l'Épitaphe, Besançon 25030
42		e-mail	
<hr/>			
43		Family Name	Liu
44		Particle	
45		Given Name	B.
46		Suffix	
47	Author	Organization	Southwest Jiaotong University
48		Division	School of Mechanics and Engineering
49		Address	Chengdu 610031
50		e-mail	
<hr/>			
51		Received	1 August 2016
52	Schedule	Revised	
53		Accepted	22 December 2016
<hr/>			
54	Abstract	The sintering of 17-4PH stainless steel powder using microwaves has rarely been reported with results better than those produced by sintering with conventional resistive heating. This study evaluates the effect of the sintering temperature, holding time, heating rate and the pre-sintering stage in microwave-assisted sintering. By optimizing the sintering step to determine the optimal process, a more homogeneous microstructure, a greater sintered density, a greater shrinkage and better mechanical properties were obtained using microwave-assisted sintering. The total process time of the microwave-assisted sintering was notably less than conventional sintering, and the peak temperature was 150 to 200 °C lower. In 17-4PH stainless steel powder, microwave-assisted sintering was demonstrated to produce significantly better mechanical properties than conventional sintering. Measurements of the hardness distribution within the sintered specimen described the gradient of	

the mechanical properties of the microwave-sintered components. This study highlights why PM 17-4PH stainless steels should be produced using microwave-assisted sintering.

55	Keywords separated by ' - '	Microwave-assisted sintering - Powder injection moulding - Heating rate - Gradient in mechanical properties - 17-4PH
56	Foot note information	

Sintering of 17-4PH stainless steel powder assisted by microwave and the gradient of mechanical properties in the sintered body

J. Shi^{1,2,3} · Z. Cheng² · J.C. Gelin³ · T. Barriere³ · B. Liu²

Received: 1 August 2016 / Accepted: 22 December 2016
© Springer-Verlag London 2017

Abstract The sintering of 17-4PH stainless steel powder using microwaves has rarely been reported with results better than those produced by sintering with conventional resistive heating. This study evaluates the effect of the sintering temperature, holding time, heating rate and the pre-sintering stage in microwave-assisted sintering. By optimizing the sintering step to determine the optimal process, a more homogeneous microstructure, a greater sintered density, a greater shrinkage and better mechanical properties were obtained using microwave-assisted sintering. The total process time of the microwave-assisted sintering was notably less than conventional sintering, and the peak temperature was 150 to 200 °C lower. In 17-4PH stainless steel powder, microwave-assisted sintering was demonstrated to produce significantly better mechanical properties than conventional sintering. Measurements of the hardness distribution within the sintered specimen described the gradient of the mechanical properties of the microwave-sintered components. This study highlights why PM 17-4PH stainless steels should be produced using microwave-assisted sintering.

Keywords Microwave-assisted sintering · Powder injection moulding · Heating rate · Gradient in mechanical properties · 17-4PH

✉ T. Barriere
thierry.barriere@univ-fcomte.fr

¹ School of Civil Engineering and Architecture, Southwest University of Science and Technology, Mianyang 621010, China

² School of Mechanics and Engineering, Southwest Jiaotong University, Chengdu 610031, China

³ UBFC, Department of Applied Mechanics, Femto-ST Institute, Besançon, 24 Rue de l'Épitaphe, 25030 Besançon, France

1 Introduction

17-4PH stainless steel is a type of martensitic precipitation-hardened material with high-performance mechanical properties [1]. Via heat treatment, high yield strengths of up to 1300 MPa can be achieved. With its excellent corrosion resistance, this versatile material is widely used in the aerospace, chemical, petrochemical, food processing, nuclear and general metalworking industries. Most studies related to the sintering of 17-4PH stainless steel have investigated conventional resistive heating (CRH); for example, Ye et al. [2] investigated the densification behaviour of this material at 650–1050 °C. Sung et al. investigated the effect of sintering kinetics by tensile testing micropowder injection moulding (PIM) 17-4PH specimens and specifically tested the influence of the cooling stage on the microstructural, tensile and fatigue properties. The results were compared with conventionally produced 17-4PH products [3]. The combination of 17-4PH stainless steel powder with a rubber binder provides increased mechanical properties of the sintered specimens. The optimal heating rate of 5 °C/min during sintering results in a greater density, greater tensile strength, less porosity and a more homogenous grain shape morphology [4].

17-4PH powders have been used in powder injection moulding, which is a type of the powder metallurgy, to create fully dense or porous components with functional properties. For example, Mutlu and Oktay [5] successfully used the space holder technique and CRH sintering to produce highly porous 17-4PH stainless steel with porosities between 39 and 82%. Suri et al. [6] performed Charpy V-notch impact tests on full-sized and small specimens to describe the impact properties of sintered and wrought 17-4PH stainless steel. Simchi et al. [7] experimented with a bilayer structure and discovered that the strain rate of 17-4PH was greater than 316L during sintering. Imgrund et al. [8] also produced magnetic-non-magnetic bimetallics made from

66 316L/17-4PH and 316L/Fe powders using micrometal injection
67 moulding and the CRH sintering process.

68 Microwave (MW) heating results from the absorption of
69 the energy transported from an oscillating electromagnetic
70 field [9]. This absorption manifests as molecular vibrations
71 (i.e., rotating electric dipole/dipole reorientations) and ionic
72 conduction in the sintered materials. The absorbed energy is
73 transformed into heat, which sinters the powdered material. At
74 low temperatures, the metal powder exhibits poor coupling
75 with the microwaves [10]. The MW-assisted sintering is a
76 process in which the sintered material absorbs the electromag-
77 netic energy from microwaves. The furnaces that are typically
78 used for MW-assisted sintering operate at a frequency of
79 2.45 GHz, while the reported tests were measured at greater
80 than 8.0 GHz. The primary advantages of MW-assisted
81 sintering are detailed as follows: rapid densification kinetics,
82 reducing the required time and energy, rapid internal heating
83 [11], lower peak temperature [12], finer microstructures and
84 improved mechanical properties [13]. To apply MW-assisted
85 sintering, many studies investigated different powder materi-
86 als. Chockalingam et al. have investigated the phase trans-
87 formation, microstructure and mechanical properties of two
88 MW-assisted sintering materials: silicon nitride (Si_3N_4) with
89 lithium yttrium oxide (LiYO_2) and zirconia (ZrO_2) sintering
90 additives [14] and β -SiAlON-ZrO₂ composites [15]. Bykov
91 et al. [16] investigated the influence of MW heating on mass
92 transport phenomena and phase transformations in nanostruc-
93 tured ceramic materials. Chandrasekaran et al. [17] conducted
94 MW heating and melting of lead, tin, aluminium and copper
95 with a silicon carbide susceptor. Srinath et al. [18] illustrated a
96 novel method to join bulk metallic materials with high thermal
97 conductivities, such as copper, using MW heating. Panda et al.
98 [19] compared the effect of the heating mode on the densifi-
99 cation, microstructure, strength and hardness of austenitic
100 (316L) and ferritic (434 L) stainless steels. The advantages
101 of MW-assisted sintering were all confirmed in these studies.

102 For the magnetic induction of sintered powder in microwave
103 heating, not all the metallic materials interact with the magnetic
104 fields. The non-ferrous metals, as well as some stainless steels in
105 austenitic structures, are not inducible to magnetics. However, 17-
106 4PH stainless steel is a magnetic inducible material. Only one
107 study that investigated the MW processing of 17-4PH stainless
108 steel powder was found in the literature. That study was a prelim-
109 inary investigation performed by Bose et al. [20], and the results
110 indicated that MW-assisted sintering did not improve the mechan-
111 ical properties of the 17-4PH stainless steel compared to CRH
112 sintering. Thus, more research must be performed regarding the
113 properties of 17-4PH stainless steel using MW-assisted sintering.

114 In common practice, the MW sinterability of a material is
115 determined from many factors; the dominant factors are the
116 sintering process' parameters, which include the sintering tem-
117 perature, the holding time, the heating rate and the pre-sintering
118 stage [21]. The sintering atmosphere also has an important

119 impact on the corrosion behaviour and mechanical properties
120 of the resulting material. Stainless steel powders should be
121 sintered in hydrogen or argon atmospheres with low dew points
122 or in a vacuum to reduce oxidation [22]. The particle size of the
123 powder is also an important factor; powders with smaller parti-
124 cles produce denser materials with higher performance mechan-
125 ical properties [23]. Some recent studies using compact 316L
126 stainless samples have illustrated the effects of the heating rate
127 used in microwave-assisted sintering on the densification, tensile
128 strength and elongation of the sintered results [23]. The use of
129 finer stainless steel powders improves the physical and mechan-
130 ical properties of the samples sintered using both methods [23].

131 The authors established a complete frame of simulation for
132 MW-assisted sintering using COMSOL software that included
133 heat generation in the powder due to the microwaves and the
134 densification of the sintered components [24]. This simulation
135 frame was built using test data: the multi-physics modelling and
136 simulation of MW heating [25], the simulation of the heat trans-
137 fer in the sintered body and the sintering behaviours described in
138 a previous study [26]. The constitutive law for sintering stainless
139 steel powders could be integrated using COMSOL through the
140 User subroutine; however, this subroutine does not consider the
141 electromagnetic properties of stainless steel powders at different
142 temperatures or at different relative densities. The measurement
143 of the complex permittivity and permeability on magnetic stain-
144 less steel powder is also required within the filler of the MW
145 absorber composite. This measurement, however, does not accu-
146 rately describe the MW-assisted sintering of nearly pure stain-
147 less steel powder after debinding [27]. A measurement was taken
148 based on barium and strontium ferrite powders, but the frequency
149 used was markedly greater than the frequency used in the furnace
150 for MW-assisted sintering [28].

151 To better understand the sintering properties of 17-4PH stain-
152 less steel, this study examined the densification and the micro-
153 structure evolution of 17-4PH stainless steel powder produced
154 using MW-assisted sintering. The injected specimens were sub-
155 jected to 2.45 GHz microwaves in a multi-mode furnace, and the
156 effects of different processing factors during sintering were in-
157 vestigated. After solid-state sintering, the evolution of the micro-
158 structure, the densification and the mechanical response of
159 sintered specimens were studied by analysing the Vickers hard-
160 ness and ultimate tensile stress. A comparison of materials pro-
161 duced using MW-assisted sintering and the CRH process was
162 also performed.

163 2 Experimental procedure

164 2.1 Materials

165 The experimental specimens were made of water-atomized
166 commercial AISI 17-4PH stainless steel powder with an aver-
167 age particle size of 11 μm . The water-atomized particles had

168 irregular shapes. The chemical composition of the 17-4PH
 169 stainless steel used in this study is shown in Table 1 and was
 170 based on standard AISI630.

171 **2.2 Process description of debinding and sintering stages**

172 In this study, the green portions of the 17-4PH stainless steel
 173 powders were prepared via several processes before MW-
 174 assisted sintering. The stainless steel powders were first mixed
 175 with wax-based thermoplastic binders based on the appropri-
 176 ate polymer–powder formulations that were optimized by
 177 Kong et al. [29] and were then formed with injection mould-
 178 ing equipment. The density of the green portions was approx-
 179 imately 5.05 g/cm³, which was 64% of the density of pure 17-
 180 4PH stainless steel (7.89 g/cm³).

181 The binder in the injected specimen was almost completely
 182 removed during the two debinding stages using sequential
 183 solvent and thermal methods [30, 31]. Before sintering,
 184 binders were debound in an argon atmosphere to prevent ox-
 185 idation. An electric thermal debinding oven was used. The
 186 first stage was to remove the water vapour held within the
 187 powder. The injected components were thus heated from 20
 188 to 130 °C at a heating rate 55 °C/h; this temperature is lower
 189 than the decomposition temperature of the paraffin wax. Then,
 190 the temperature was increased up to 220 °C at a slower heating
 191 rate of 4.5 °C/h to remove the paraffin wax. The specimens
 192 were then cooled for 2 h to the ambient temperature. This
 193 debinding cycle was also used by Quinard et al. [30] when
 194 studying PIM feedstock with 316L stainless steel powder
 195 (mean particle size = 3.4 µm) to investigate the
 196 microcomponents. In powder metallurgy, finer starting pow-
 197 der particles are known to have better sinterability and, there-
 198 fore, tend to achieve relatively greater sintered densities.
 199 During the debinding process, the weight of the specimens
 200 was reduced by 6.3%. This preliminary debinding stage was
 201 necessary to prevent cracking in the next sintering stage [31].

202 The research of Quinard et al. [30], who investigated the
 203 CRH sintering of 316L stainless steel, was used as a reference
 204 for the experimental set-up used in this study. The heating
 205 processes included three steps. First, the specimens were heat-
 206 ed to 600 °C and held at that temperature for 30 min to
 207 completely remove the remaining binder components. Then,
 208 the temperature was increased to 900 °C and held again for
 209 30 min. Finally, the temperature was increased to the peak
 210 value of the prescribed test and then held again for 10 min.
 211 It was expected that during the heating process, the residual

212 binder would continue to decompose, leading to a decrease in
 213 weight. The weight gain during sintering with an increase in
 214 the temperature implied that some reactions in addition to the
 215 decomposition of the residual binder had occurred during
 216 sintering.

217 The schematic illustration of all of the steps (i.e., from
 218 powder particles to sintered parts) is shown in Fig. 1. The
 219 experiments in this paper show that the pre-sintered specimens
 220 of the compacted 17-4PH stainless steel powder possess the
 221 necessary initial stiffness for the beginning of the sintering
 222 process. The final sintering stage is represented by two possi-
 223 ble methods: CRH or MW-assisted sintering.

224 A high-temperature microwave laboratory system
 225 (HAMilab-V1500, 2.45 GHz) was used in this study,
 226 based on a multi-mode microwave cavity. The continu-
 227 ously adjustable microwave power varied from 0.2 to
 228 1.35 kW. The maximum working temperature was
 229 1600 °C, and the maximum heating rate could exceed
 230 50 °C/min. The surface temperature of the specimen was
 231 continuously measured using a high accuracy Raytek IR py-
 232 rometer from an exterior cavity window. The IR sensor detects
 233 the temperature from 600 to 1600 °C, and the temperature
 234 accuracy is approximately ±0.5%. The precision of the mea-
 235 surement is subject to many factors, including the sample size
 236 and its surface quality, the emissivity according to the material
 237 composition, the sample IR pyrometer alignment, the varia-
 238 tion of emissivity with temperature, etc. The pyrometer mea-
 239 sures the radiant energy from the sample surface and deter-
 240 mines the temperature based on a preset emissivity. The tem-
 241 perature measurements for all the compacted powder speci-
 242 mens were made based on the preset emissivity of steel (0.35)
 243 [32]. The MW heating behaviour of metal powder compact is
 244 influenced by a few factors, including the design of the MW
 245 cavity, the physic properties of the materials, the number of
 246 samples and their position in the cavity, etc. A flat SiC was
 247 placed under the compacted powder, and certain chopped
 248 susceptors were placed around the powder based on the re-
 249 search by Kim-Hak et al. [33].

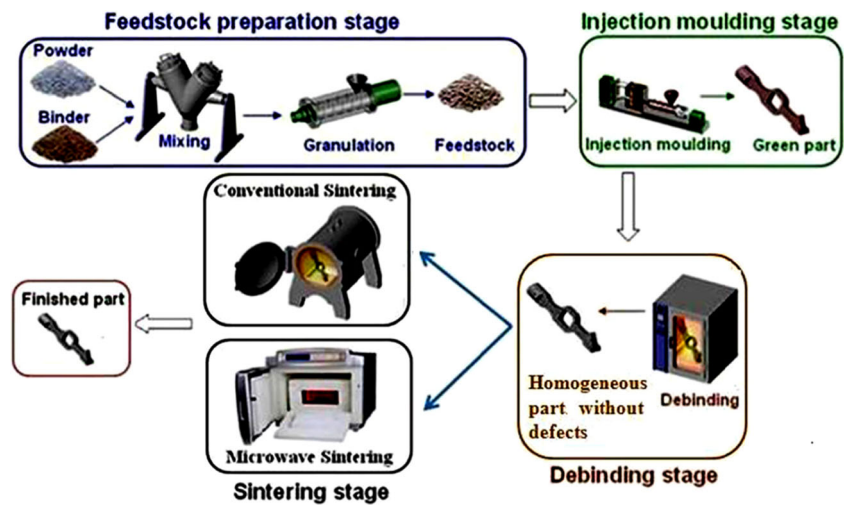
250 To study the densification behaviour at different heating
 251 modes, the same debound components were also sintered
 252 using CRH in a vertical SETSYS® SETARAM evolution
 253 analyser. The dilatometer sintering CRH tests, in an analyser,
 254 have been performed in a primary vacuum of approximately
 255 10⁻³ mbar. The MW-assisted sintering tests were performed in
 256 argon atmosphere due to the atmosphere control of the micro-
 257 wave laboratory system.

t1.1 **Table 1** Chemical composition
 t1.2 of 17-4PH stainless steel (wt%)

Fe	Ni	Cr	C	Cu	Nb	Mn	S	P	Si
71.8–73.8	3.0–3.5	15.5–17.5	≤0.07	3.0–5.0	0.45	≤1.0	≤0.03	≤0.04	≤1.0

t1.3

Fig. 1 Sequential stages to obtain the final sintered parts. The sintering stage can be processed using the CRH or MW methods



258 **2.3 Sizes of the specimens after being injected, debound**
 259 **and undergoing MW-assisted sintering**

260 The sizes of the specimens after being injected, debound and
 261 undergoing MW-assisted sintering were measured and compared,
 262 as shown in Fig. 2, and exhibit marked shrinkages after
 263 sintering (e.g., approximately 15% along the *x*-direction).

264 **2.4 Material characterization of the sintered specimens**

265 To evaluate the results of the sintering process, certain mea-
 266 surements and observations were performed and analysed.
 267 The shrinkage of the sintered specimens was measured using
 268 callipers, and the bulk densities of the specimens were tested
 269 using Archimedes' principle. For the measurements, the sam-
 270 ples were immersed into an ethanol-based liquid; then, two
 271 sets of sintered samples that had been sintered under the same
 272 sintering conditions were wet-polished using a manual polish-
 273 er. One set was used to measure the hardness distribution in
 274 the sintered body; the polished section was in the middle plane
 275 of the sintered component with nearly half of the body re-
 276 moved. The other set was used to observe and analyse the
 277 material's microstructures; the polished section was near the
 278 exterior surface, and only a thin layer of the sintered material
 279 was removed to expose and prepare this section. The

distribution of the Vickers bulk hardness in the middle section
 280 of the sintered body was measured at nine locations arranged
 281 equidistantly along two perpendicular directions (i.e., *x* and *y*).
 282 The measurements were performed using a 5-kg load and a
 283 10-s duration. To obtain reliable measurements, the hardness
 284 at each location was recorded as the average of five readings
 285 near the location on the prepared section of the middle plane.
 286

For clear observations, the observed areas of the specimens
 287 were polished and chemically etched. Metallographic process-
 288 es were used in the microstructural analyses, and a 4% nitric
 289 acid solution and alcohol were used to etch the polished sur-
 290 face. Next, an optical microscope was used to observe the
 291 microstructure of the polished and chemically etched speci-
 292 men surfaces.
 293

294 **3 Results and discussion**

295 **3.1 Important factors in the MW-assisted sintering process**

296 *3.1.1 Peak sintering temperature*

297 The optimal peak temperature of the MW-assisted sintering of
 298 the 17-4PH stainless steel powder is expected to be less than
 299 the peak temperature of CRH sintering. To determine the ef-
 300 fect of the peak temperature on the sintering results, tests were
 301 performed at different peak temperatures, while other process-
 302 ing factors remained the same. Therefore, any variation in the
 303 results was affected only by the change in the peak tempera-
 304 ture. The debinding and pre-sintering kinetics have been de-
 305 scribed in paragraph 1.2. The same heating rate of 5 °C/min
 306 was used, and the specimen was held at the peak temperature
 307 for 10 min in all test processes, and the results produced by the
 308 different peak temperatures are shown in Table 2.

309 Table 2 shows that a suitable peak temperature will result in
 310 optimized results. For the MW-assisted sintering of the 17-

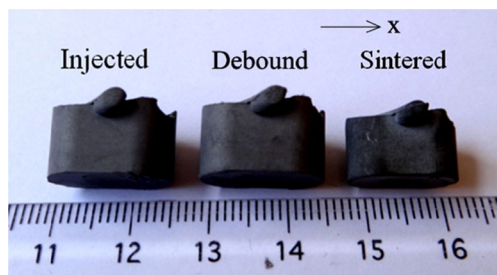


Fig. 2 Size comparison after injection moulding, thermal debinding and MW-assisted sintering of 17-4PH stainless steel powder specimens

t2.1 **Table 2** Comparison of the shrinkages along the *x*-direction (shown in Fig. 2), the relative densities and the Vickers hardnesses

t2.2	Peak temperature (°C)	Size shrinkage (%)	Relative density (%)	Vickers hardness (HV)
t2.3	1100	5.67 ± 0.5	72.6 ± 0.11	173 ± 3
t2.4	1140	10.29 ± 0.4	90.5 ± 0.06	280 ± 4
t2.5	1150	12.47 ± 0.08	90.9 ± 0.04	311 ± 2
t2.6	1160	9.98 ± 0.2	86.7 ± 0.07	235 ± 3
t2.7	1200	8.12 ± 0.15	81.2 ± 0.05	267 ± 2

The values were obtained from specimens sintered at different peak temperatures. All processes used a heating rate of 5 °C/min, and the specimen was held at the peak temperature for 10 min

311 4PH stainless steel powder, the optimal peak temperature is
 312 shown to be 1150 °C, which results in a greater sintered density
 313 and better mechanical properties. This increase in the
 314 relative density may be caused by the decrease in the number
 315 of pores within the material, and the decline in the relative
 316 density with a peak sintering temperature greater than
 317 1150 °C may be caused by the non-uniformity of the grain
 318 growth within the material, which increases the material's
 319 open porosity [34].

320 **3.1.2 Holding time**

321 In the second tests, all samples were sintered to the same peak
 322 temperature of 1150 °C, which was the optimal peak temper-
 323 ature determined by the first tests. The durations of the holding
 324 time at the peak temperature were changed for each of these
 325 tests, while other processing factors were held constant to
 326 exclude the effects of other factors. Under this condition, the
 327 sintering results for different holding times are shown in
 328 Table 3.

329 The results shown in Table 3 indicate that an optimal
 330 heating duration exists for the peak temperature in MW-
 331 assisted sintering. With 17-4PH stainless steel powder, a hold-
 332 ing time of 10 min is shown to produce the greatest density
 333 and best mechanical properties. With CRH sintering, an opti-
 334 mal holding duration also exists. Shorter holding times are
 335 shown to be insufficient for proper densification, while longer
 336 durations may lead to grain coarsening [29].

337 **3.1.3 Heating rate**

338 For the third group of the tests, the heating rates were varied.
 339 The optimal peak temperature (1150 °C) and holding time
 340 (10 min) identified earlier were used as the optimal values
 341 determined by two previous sets of tests. To investigate the
 342 effects of the heating rate in detail, the specimens were heated
 343 directly to the peak temperature from the ambient temperature
 344 and were held there for 10 min. The heating rates were set at
 345 different values in different tests, and the results of the MW-

assisted sintering for different heating rates are shown in 346
 Table 4. 347

348 From the results in Table 4, a heating rate of 50 °C/min 348
 349 damaged the specimen; thus, a heating rate that is too high can 349
 350 produce an uneven temperature distribution within the mate- 350
 351 rial and can lead to the distortion or collapse of the material. A 351
 352 heating rate of 30 °C/min was shown to be optimal for the 352
 353 MW-assisted sintering of 17-4PH stainless steel. Based on 353
 354 reference [23], different shrinkage rates and different physical 354
 355 properties are the results of different porosities in MW- 355
 356 sintered samples. The porosity depends on the heating rate; 356
 357 thus, it is reasonable that the shrinkage, the relative density 357
 358 and the Vickers hardness also depend on the heating rate. At a 358
 359 heating rate of 30 °C/min during the MW-assisted sintering of 359
 360 17-4PH stainless steel powders, the lowest porosity was ob- 360
 361 tained, resulting in a greater density and a greater hardness in 361
 362 the sintered specimens. 362

363 **3.1.4 Pre-sintering temperature**

364 Based on the above-mentioned results, specimens were heated 364
 365 to the peak temperature of 1150 °C at a heating rate of 365
 366 30 °C/min and were then held at the peak temperature for 366
 367 10 min. Then, the pre-sintering stage of the sintering process 367
 368 was analysed. Before the formal sintering stage, the specimens 368
 369 were heated to a pre-sintering temperature and then held for 369
 370 30 min. The results for different pre-sintering temperatures are 370
 371 shown in Table 5. A test without pre-sintering was also per- 371
 372 formed for comparison with the other processes. 372

373 In Table 5, the best result was obtained by the process without 373
 374 the pre-sintering stage. If pre-sintering is necessary to obtain a 374
 375 given initial stiffness, a lower temperature should be used to 375
 376 produce a better quality material. The primary role of pre- 376
 377 sintering is to provide an initial stiffness for the initial stage of 377
 378 sintering. In some case, rapid heating induces inhomogeneities in 378
 379 the temperature; thus, the sintered specimen requires a given 379
 380 initial strength to prevent distortion or damage when sintering 380
 381 begins. Pre-sintering is thus unnecessary and provides no bene- 381
 382 ficial effect. 382

t3.1 **Table 3** Comparison of the shrinkages along the *x*-direction (Fig. 2), the relative densities and the Vickers hardnesses

t3.2	Holding time (min)	Size shrinkage (%)	Relative density (%)	Vickers hardness (HV)
t3.3	5	8.81 ± 0.3	85.9 ± 0.08	238 ± 1
t3.4	10	12.47 ± 0.1	90.9 ± 0.03	311 ± 2
t3.5	15	8.32 ± 0.25	84.6 ± 0.1	253 ± 2
t3.6	20	8.19 ± 0.4	83.4 ± 0.14	277 ± 3

The values were obtained from the specimens sintered using MW with different holding times for the same peak temperature. All processes used a heating rate of 5 °C/min, and all specimens were sintered at the same peak temperature of 1150 °C

t4.1 **Table 4** Comparison of the shrinkages along the x-direction (Fig. 2), the relative densities and the Vickers hardnesses

t4.2	Heating rate (°C/min)	Size shrinkage (%)	Relative density (%)	Vickers hardness (HV)
t4.3	10	11.11 ± 0.33	92 ± 0.15	227 ± 2
t4.4	20	15.15 ± 0.15	95 ± 0.08	299 ± 2
t4.5	30	16.11 ± 0.07	96.6 ± 0.05	316 ± 1
t4.6	40	14.90 ± 0.55	93.6 ± 0.20	231 ± 5
t4.7	50	Specimen damaged		

The values were obtained from specimens sintered using MW at different heating rates. All processes sintered the material at the same peak temperature of 1150 °C, and the material was held at the peak temperature for 10 min

383 A conclusion can be drawn from the facts mentioned in
 384 Sect. 2: The optimal choice for the MW-assisted sintering
 385 process for a compacted specimen of 17-4PH stainless steel
 386 powder with a powder size near 11 µm is shown in Fig. 3.

387 **3.2 Microstructure**

388 Sintered metal injection moulding (MIM) parts are expected
 389 to have some residual porosity and typically have densities
 390 ranging from 95 to 99% of the theoretical density. A finer
 391 starting powder particle size is observed, in general, to result
 392 in finer pores.

393 The microstructures of the sintered materials in this study
 394 have been observed using optical microscope. The sintering
 395 stage was interrupted at different temperatures from 950 to
 396 1150 °C and left to cool to allow observation of the corre-
 397 sponding microstructures. When the peak temperature was
 398 achieved, a holding time of 10 min was maintained. The evo-
 399 lution of the micrographs from powders to the sintered mate-
 400 rial is shown in Fig. 4a–f.

401 Figure 4 shows the evolution of the particle crystallization.
 402 When sintered to 950 °C, the material just began the sintering

t5.1 **Table 5** Comparison of the shrinkages along the x-direction (Fig. 2), the relative densities and the Vickers hardnesses

t5.2	Pre-sintering temperature (°C)	Size shrinkage (%)	Relative density (%)	Vickers hardness (HV)
t5.3	900	9.33 ± 0.45	83.7 ± 0.04	182 ± 2
t5.4	600	10.12 ± 0.55	87.8 ± 0.13	190 ± 2
t5.5	400	12.15 ± 0.35	89.9 ± 0.08	207 ± 3
t5.6	270	13.94 ± 0.08	93.4 ± 0.10	274 ± 1
t5.7	No pre-sintering stage	16.11 ± 0.10	96.6 ± 0.05	316 ± 2

The values were obtained from the specimen sintered using MW at different pre-sintering temperature. For all processes, the specimen was heated at the same heating rate of 30 °C/min up to the same peak temperature of 1150 °C and held at the peak temperature for 10 min

process. The samples are shown to be porous and be com- 403
 posed of small grains. As the sintering temperature increased, 404
 the number of pores decreased, and the rate of grain growth 405
 markedly increased. From Fig. 4d, f, marked grain growth 406
 is shown; most of the larger pores are located at the grain bound- 407
 ary. This phenomenon is favourable for the evacuation of gas 408
 entrapped in the porous powder compact and for the densifi- 409
 cation process. When the temperature reached 1150 °C 410
 (Fig. 4f), relatively larger pores that were not particularly uni- 411
 formly distributed were nearly eliminated; this phenomenon 412
 relates well to the mechanical properties of the final samples. 413

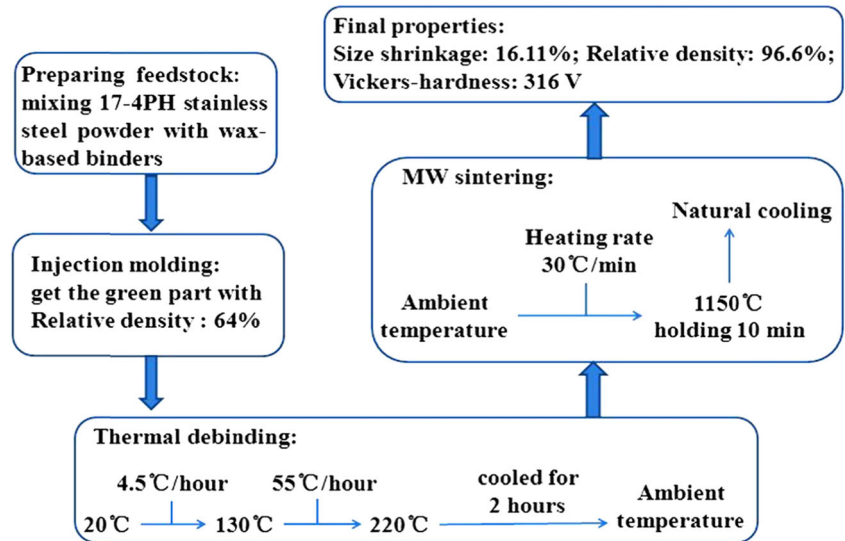
414 **3.3 Distribution of the Vickers hardness**

During MW processing, heat is produced inside the bulk ma- 415
 terial and sent out via radiation and convection from the outer 416
 surfaces of the specimens; thus, a thermal gradient occurs. 417
 During the MW heating of the sintering process, the temper- 418
 ature in the core is generally greater than the temperature on 419
 the surface. The outer surface at different positions on the 420
 specimen is, thus, subjected to different temperatures due to 421
 the irregular shape of the sintered body. The sintered material 422
 closer to the centroid becomes denser and generally exhibits 423
 better mechanical properties; this phenomenon can be demon- 424
 strated by detection of the hardness distribution over the 425
 polished cross section of the specimen. 426

The hardness distribution on a plane section was measured 427
 using a specialized procedure. A cross section near the middle 428
 plane of the specimen was prepared. On the polished section 429
 plane, nine small areas were arranged along the horizontal and 430
 vertical axes, as shown in the legend in the top right corner of 431
 Figs. 5 and 6. These areas were labelled in sequence from ×1 432
 to ×5 and from y1 to y5. In each small area, five spots were 433
 tested. The average value of the five test results was recorded 434
 as the formal hardness of the small area. 435

As expected, the experimental results in Figs. 5 and 6 dem- 436
 onstrate the nature of MW-assisted sintering. The values at 437
 symmetrical positions (e.g., left and right or up and down) 438
 are shown to not be symmetric. The asymmetry in the values 439
 of the Vickers hardness was induced via hybrid MW-assisted 440
 sintering. For example, points y4 and y5 in the lower half were 441
 closer to the susceptor than points y2 and y1 in the upper half. 442
 Their closer location relative to the assisted heating SiC ma- 443
 terial resulted in greater heating rates and greater Vickers hard- 444
 ness values. It appears reasonable to claim that the contribu- 445
 tion of the magnetic field is more important than the contribu- 446
 tion of the electric field. However, the main contribution to the 447
 sample heating is due to the infrared radiation of the SiC 448
 susceptors. The SiC screens partially block the electromagnet- 449
 ic fields. The SiC susceptors play an auxiliary role in micro- 450
 wave heating. The physical properties of 17-4PH stainless 451
 steel powder are not sufficient to provide coupling with the 452
 electromagnetic field at a low temperature. The impact by 453

Fig. 3 Optimal process proposed for the MW-assisted sintering of specimens made of compacted 17-4PH stainless steel powder



454 microwave directly on the heating of the powder is very dif- 456 property of powder compact can be altered by increasing the 456
 455 ficult due to the departure from a cold state. However, the 457 temperature. The effective heating of the test sample occurs 457

Fig. 4 Micrographs of the microstructure evolution for the MW-assisted sintering of the 17-4PH stainless steel powder observed using optical microscope: MW-assisted sintering at **a** 950 °C, **b** 1000 °C, **c** 1050 °C, **d** 1100 °C, **e** 1140 °C, **f** 1150 °C and held for 10 min

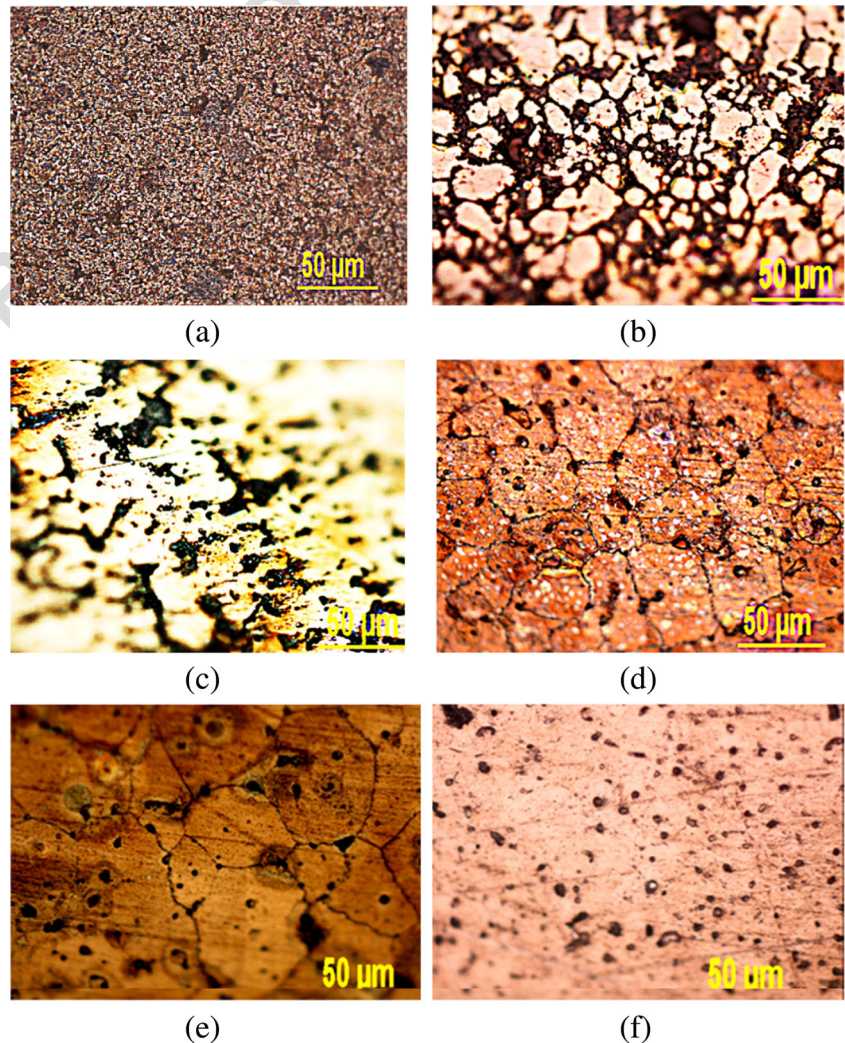
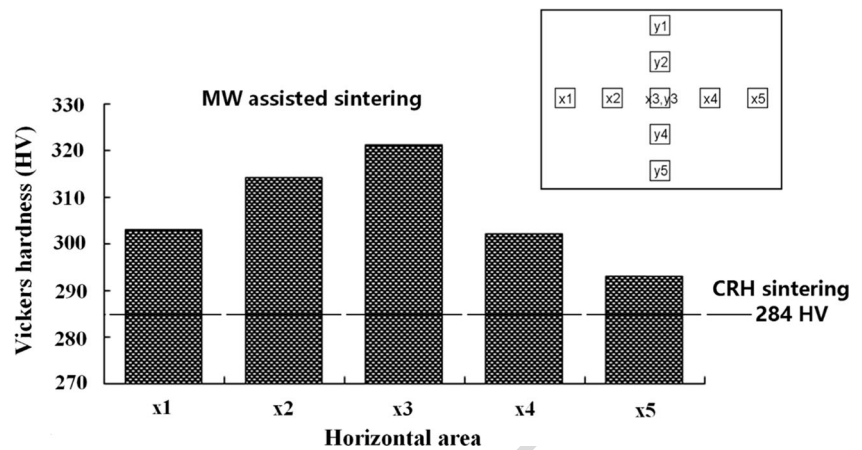


Fig. 5 Vickers hardness values for each small area along the horizontal direction



458 after the pre-heating or auxiliary heating using the SiC
 459 susceptors, when its properties become sufficient to provide
 460 a strong induction at a relatively higher temperature. Then, the
 461 effective heating is produced inside the powder impact for the
 462 true sintering process. As an auxiliary heating source, the SiC
 463 susceptors play another role to homogenize the temperature in
 464 the furnace cavity.

465 The difference in the hardness values among these small
 466 areas is approximately 20 to 30 Vickers units within such a
 467 small area. The gradient of the mechanical properties is also
 468 known to be significant in the sintered bodies; this phenom-
 469 enon is caused by the rapid heating that occurs during the MW-
 470 assisted sintering due to the heat produced within the material.
 471 However, there is no available method that can slow the opti-
 472 mal heating rate; lower heating rates result in worse sintering
 473 qualities due to grain coarsening. This is an important fact that
 474 is demonstrated in the experimental results above. Thus, the
 475 gradient of the mechanical properties in the sintered bodies
 476 can be considered to be commonly produced by MW-assisted
 477 sintering and represents an important phenomenon to study
 478 the relationship between the evolution of the temperature gra-
 479 dient and the gradient of the mechanical properties in the

480 sintered products. The prediction of gradient in the mechani-
 481 cal properties shows its potential value in studies of function-
 482 ally graded materials. Further research on the modelling and
 483 simulation of these property gradients in MW-assisted
 484 sintering bodies should be performed.

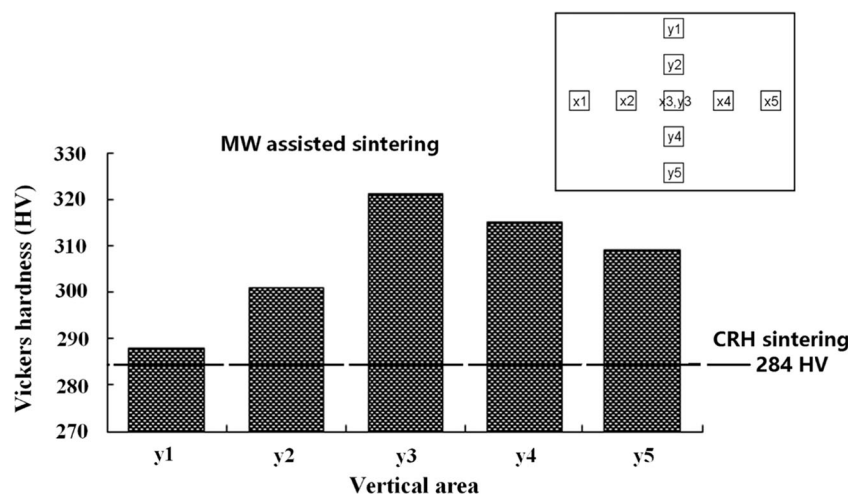
485 None of the MW-sintered specimens in this study exhibited
 486 visually observable distortions. Because the shape of the stud-
 487 ied specimens was not sensitive to distortion and because no
 488 precise measurement was applied to their geometries, this
 489 conclusion is just an estimate. The influence of the tempera-
 490 ture gradient on the shape of the distortion of sintered bodies
 491 should be determined using specially designed specimens
 492 with precise measurement of their geometries.

3.4 Comparison with conventional sintering

3.4.1 Sintering of 17-4PH stainless steel using conventional sintering (CRH)

493
 494
 495
 496 To study and compare the densification behaviours of the
 497 different sintering processes described in this study, the same
 498 debound components were sintered using CRH sintering in a

Fig. 6 Vickers hardness values for each small area along the vertical direction



vertical SETSYS® SETARAM evolution analyses. These specimens were heated to a peak temperature of 1350 °C at heating rates of 5, 10, 20 and 30 °C/min and then were held for 2 h. Based on the process proposed by Song [26], the temperature was held for 30 min when it reached 600 and 900 °C to ensure the homogenization of the temperature in the sintered bodies. The evolutions of the shrinkages and the shrinkage rates versus the temperature are shown in Fig. 7.

3.4.2 Comparison of MW and CRH sintering

Based on the conclusion results in Sect. 2.1.4, two tests were used for comparison. For the CRH sintering, the specimens were heated to 1350 °C at a heating rate of 5 °C/min and held at this temperature for 2 h. During the heating process, the temperature was held for 30 min when it reached 600 and 900 °C, respectively. For MW-assisted sintering, specimens were heated directly to 1150 °C at a heating rate of 30 °C/min and held at this temperature for 10 min. These test parameters were optimal, as determined above.

Table 6 shows the following: (1) The sintering of compacted 17-4PH stainless steel powder in an MW furnace reduces the required processing time by 90%; (2) the optimal peak temperature for the MW-assisted sintering is between 150 and 200 °C less than the optimal temperature for the CRH sintering; and (3) the achieved shrinkage, relative density and hardness of the MW-sintered materials are greater than the properties obtained using the CRH sintering according to a dilatometer. Similar results were obtained by Charmond [12], whose study showed that MW-sintered specimens in Y-tetragonal zirconia polycrystal powder exhibited a greater final density than the CRH-sintered specimens at the same temperature. A reasonable interpretation of the positive effect of the MW on the densification of the powder materials is the non-thermal effects of the microwaves, which are induced by high-frequency electromagnetic fields.

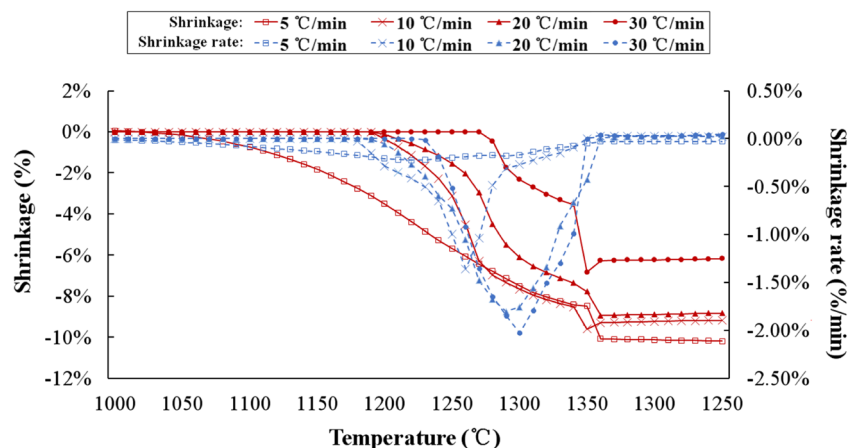
During a conventional sintering process, a high heating rate results in a thermal gradient within the compacts followed by a

distortion and inhomogeneous microstructure in the sintered bodies. A slower heating rate was applied when using the isothermal holdings to achieve a stepwise variation of the temperatures. This represents a longer process time and greater cost and provides more cause for grain coarsening in the sintered compact. In microwave-assisted sintering, microwaves interact directly with the individual particles in powder compacts. This process provides rapid heating in a volumetric manner inside the sintered compact, which, therefore, restricts the generation of grain coarsening.

Compared to CRH sintering, MW-assisted sintering has different sintering mechanisms, such as the enhancement of the diffusion coefficient [35] and the eddy current for metals [36]. Therefore, it is reasonable that the peak temperature required for MW sintering is lower than for CRH sintering.

The final microstructures of the 17-4PH stainless steel sintered using CRH sintering and MW-assisted sintering with optimal process parameters are shown in Fig. 8a, b. The grain boundaries in both the conventional and microwave-sintered specimens are not obvious. It appears that the grains finally blend together, with some residual porosity inside. The MW-assisted sintering is fast with a high heating rate and resulted in a more homogeneous microstructure with lower porosities. In MW-assisted sintering for sintering a 17-4PH stainless steel, a final temperature of 1150 °C appears to result in the most homogeneous microstructure. This temperature results in the lowest pore fraction, smallest average pore size and most spherical pore shape in the specimen sintered using MW sintering, as seen in Fig. 8a, b. Compared to the specimen sintered using MW-assisted sintering, it is clear that many more and larger gas pores are present in the specimen sintered using CRH sintering; this phenomenon is caused by the heating characteristics of CRH sintering, where heat is conducted from the outer surface into the core of the specimen. This direction of heat conduction is opposite to the outward gas exhaust. The outer layer of the powder is, thus, easier to sinter and closes its pores earlier in the sintering process, and the outer layer obstructs the paths of gas exhausting from the

Fig. 7 Shrinkage and shrinkage rate versus temperature during the sintering of 17-4PH stainless steel powder specimens at different heating rates



t6.1 **Table 6** Comparison of the
t6.2 sintering time, peak temperature
and final properties of the sintered
specimens obtained using CRH
t6.3 and MW-assisted sintering
t6.4

Sintering mode	Sintering time (min)	Peak temperature (°C)	Size shrinkage (%)	Relative density (%)	Vickers hardness (HV)
CRH	445	1350	14.95 ± 0.15	95.2 ± 0.08	284 ± 2
MW	48	1150	16.11 ± 0.10	96.6 ± 0.05	316 ± 2

573 inside the material. Some gas remains inside the specimen,
574 which then forms large pores. Compacted powder heated by
575 microwaves is more homogeneous in its microstructure, de-
576 spite the high heating rate it experiences. This phenomenon,
577 thus, exemplifies the advantage of volumetric heating provid-
578 ed by microwaves. This illustrates why specimens produced
579 by MW-assisted sintering exhibit greater densities, a more
580 homogeneous microstructure, better surface qualities and bet-
581 ter mechanical properties.

582 *3.4.3 Mechanical behaviours (Vickers hardness, ultimate*
583 *tensile stress) of MW and CRH sintering and comparison*
584 *with MPIF standard tests*

585 High-strength metallic materials are typically very sensitive to
586 small defects that locally give rise to stress concentrations.
587 The comparison of mechanical behaviours of 17-4PH as a
588 bulk and sintered material is described in Table 7. The influ-
589 ence of the mechanical properties on the initial particle size of
590 the 17-4PH stainless steel sintered using CRH sintering at
591 room temperature has been recently studied by Seerane et al.
592 [37]. In our case, for the same mean size powders, the best
593 hardness was obtained at 284 ± 2 HV, which corresponds to
594 95.2% of the relative density and is nearly equivalent to
595 280 HV and 97.5% of the relative density, which corresponds
596 to the mechanical result by Seerane et al. [37]. Figure 9 sum-
597 marizes the measured mechanical properties of the sintered
598 parts and the respective as-sintered 17-4PH stainless steel
599 minimum MPIF standard 35 specifications (MPIF, 2007).
600 However, for a comparison of the Vickers hardness, using
601 MW-assisted sintering, the minimum standard value has been
602 obtained for all directions, as seen in Figs. 5 and 6. In the case

of the best parameters, at position ×5, the high value corre-
sponding to 320 ± 5 HV is largely superior compared to the
standard MPIF value (280 ± 5 HV), as seen in Fig. 9a.

A correlation between the evolution of the hardness and the
tensile strength is in agreement with the findings by Gulsoy
et al. [38], and this relationship is also known to be common
[39, 40]. The ultimate tensile stress value, using MW-assisted
sintering, was approximately 940 MPa, as seen in Fig. 9b.
This value is superior to the MPIF requirement [41] corre-
sponding to a minimal value of 800 MPa.

The hardness and ultimate tensile stress compared to the
standard MPIF values validate the 17-4PH material properties
using the MIM and MW-assisted sintering process [37], as
seen in Fig. 9a, b.

4 Conclusions

Metal injection moulding of specimens using PM 17-4PH stain-
less steels was successfully consolidated to nearly full density
using MW-assisted sintering. The experiments in this study were
performed in a microwave laboratory system with a multi-mode
cavity. The optimal heating cycle was determined from the ex-
perimental results, and the optimal result was obtained by heating
directly from ambient temperature to 1150 °C at a heating rate of
30 °C/min and then holding the specimen at the peak temperature
for 10 min. The specimen with the greatest density (96.6%) and
best mechanical properties (Vickers hardness = 316 V, ultimate
tensile stress = 940 MPa) was achieved using these optimal
parameters. The sintered density obtained in this study was
96.6%, which is not high enough to be nearly full density. The
measured mechanical properties of the sintered parts using the
MW-assisted sintering and the respective as-sintered 17-4PH
stainless steel minimum standard MPIF specifications [39]

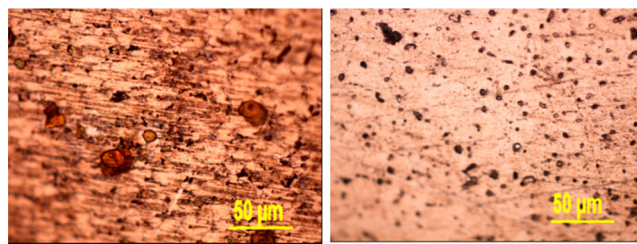


Fig. 8 Micrographs of the microstructures obtained from the specimens sintered using CRH sintering (a) and MW-assisted sintering (b)

Table 7 Comparison of the mechanical properties of the 17-4PH stainless steel at room temperature for the bulk and the sintered material

Tensile strength (MPa)	Yield strength (MPa)	Elongation (%)	Vickers hardness (kgf/mm ²)	Reference
1030	983	21	352	[42]
800			284	[41]

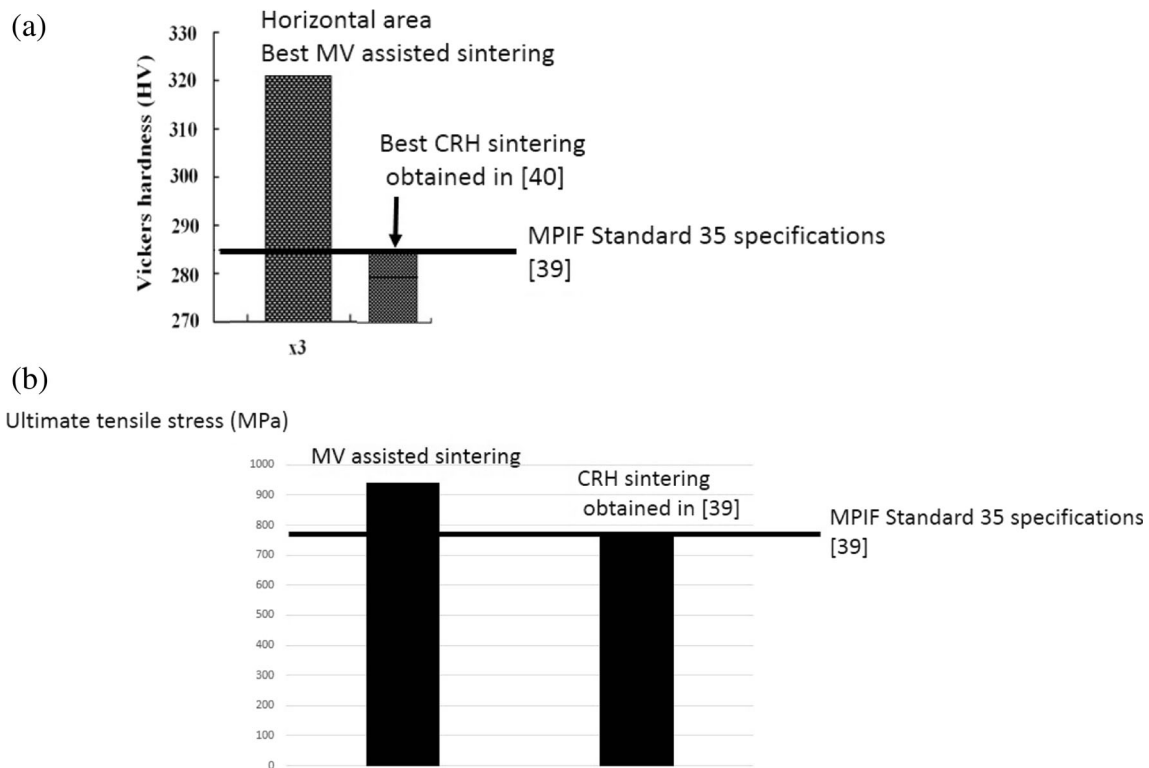


Fig. 9 The as-sintered MIM parts using CRH and MW-assisted sintering processes compared with MPIF standard 35 (Material Standard for a Metal Injection Moulded Part): **a** Vickers hardness and **b** the ultimate tensile stress

634 validate the PIM process and demonstrate the efficient and innova- 660
 635 tive MW sintering. 661

636 In this study, the results of observations and tests were 662
 637 different from results reported by Bose et al. [20]. The 663
 638 sintering of 17-4PH stainless steel powder using MW heating 664
 639 exhibited short processing times, requiring only 10% of the 665
 640 conventional sintering time to obtain better results, and lower 666
 641 peak temperatures (150 to 200 °C lower than the temperatures 667
 642 used in CRH sintering). Despite the high heating rates, the 668
 643 specimens did not show observable distortions or cracking, 669Q1
 644 which demonstrates the important advantage of volumetric 670
 645 heating using MW. This illustrates why specimens produced 671
 646 using MW-assisted sintering also result in materials with a 672
 647 greater densification, a more homogeneous microstructure, 673
 648 better surface qualities and better mechanical properties. 674
 649 When a greater density is produced, sintering using MW 675
 650 heating also results in more shrinkage. 676

651 Sintering using MW heating also results in a marked gra- 677
 652 dient in the mechanical properties of the sintered material; this 678
 653 phenomenon is induced by the rapid internal heating and the 679
 654 other physical effects that are induced by microwaves. Studies 680
 655 of this phenomenon should continue to define and describe the 681
 656 applications of MW-assisted sintering products. 682

657 Microwave-assisted sintering generally results in fast sintering 683
 658 and more homogeneous microstructures. Evidently, this explana- 684
 659 tion is not complete. More complicated physical phenomena are 685

660 still being studied to provide precise explanations. Additionally, 661
 662 modelling and simulating the generation of the gradient proper- 663
 664 ties appear to be significant for future studies. 665

666 **Acknowledgements** This work was financially supported by the National 667
 668 Natural Science Foundation of China (Grant No. 11502219) and the Doctoral 669
 669 Research Foundation of Southwest University of Science and Technology 670
 670 (Grant No. 14zx7139). The authors also wish to thank the Femto-ST Institute 671
 671 for the experimental and simulation support. 672

673 **Glossary** MW, microwave; CRH, conventional resistive heating 674

675 **References** 676Q2

677 1. Slaby SA, Kraft O, Eberl C (2016) Fatigue properties of conven- 678
 678 tionally manufactured and micro-powder-injection moulded 17-4 679
 679 PH micro-components. *Fatigue & Fracture of Engineering 680
 680 Materials & Structures* 39:649–789 681
 681 2. Ye H, Liu XY, Hong H (2008) Sintering of 17-4PH stainless steel 682
 682 feedstock for metal injection molding. *Mater Lett* 62:3334–3336 683
 683 3. Sung HJ, Ha TK, Ahn S, Chang YW (2002) Powder injection 684
 684 moulding of a 17-4PH stainless steel and the effect of sintering 685
 685 temperature on its microstructure and mechanical properties. *J 686
 686 Mater Process Techno* 130-131:321–327 687
 687 4. Jeefferie AR, Nurhashima S, Yuhazri MY, Sihombing H, Shukor 688
 688 SM, Abdullah NS, Omar MA (2011) Characterization of injection 689
 689 molded 17-4PH stainless steel prepared with waste rubber binder. 690
 690 *Journal of Mechanical Engineering and Technology* 3:11–21 691

686 5. Mutlu I, Oktay E (2011) Processing and properties of highly porous 17-
687 4 PH stainless steel. *Powder Metallurgy and Metal Ceramics* 50:73–82

688 6. Suri P, Smarslok BP, German RM (2006) Impact properties of sintered
689 and wrought 17-4 PH stainless steel. *Powder Metall* 49:40–47

690 7. Simchi A, Rota A, Imgrund P (2006) An investigation on the
691 sintering behavior of 316L and 17-4PH stainless steel powders
692 for graded composites. *Mater Sci Eng A* 424:282–289

693 8. Imgrund P, Rota A, Simchi A (2008) Microinjection moulding of
694 316L/17-4PH and 316L/Fe powders for fabrication of magnetic-
695 nonmagnetic bimetals. *J Mater Process Technol* 200:259–264

696 9. Campañone LA, Paola CA, Mascheroni RH (2012) Modeling and
697 simulation of microwave heating of foods under different process
698 schedules. *Food Bioprocess Technol* 5:738–749

699 10. Menezes RR, Souto PM, Kiminami RHGA (2007) Microwave hy-
700 brid fast sintering of porcelain bodies. *J Mater Process Technol* 190:
701 223–229

702 11. Leonelli C, Veronesi P, Denti L, Gatto A, Iuliano L (2008)
703 Microwave assisted sintering of green metal parts. *J Mater
704 Process Technol* 205:489–496

705 12. Charmond S, Carry CP, Bouvard D (2010) Densification and mi-
706 crostructure evolution of Y-tetragonal zirconia polycrystal powder
707 during direct and hybrid microwave sintering in a single-mode cav-
708 ity. *J Eur Ceram Soc* 30:1211–1221

709 13. Wu Q, Zhang X, Wu B, Huang W (2013) Effects of microwave
710 sintering on the properties of porous hydroxyapatite scaffolds.
711 *Ceram Int* 39:2389–2395

712 14. Chockalingam S, Earl DA (2010) Microwave sintering of Si₃N₄
713 with LiYO₂ and ZrO₂ as sintering additives. *Mater Des* 31:1559–
714 1562

715 15. Chockalingam S, Traver HK (2010) Microwave sintering of β-
716 SiAlON-ZrO₂ composites. *Mater Des* 31:3641–3646

717 16. Bykov Y, Egorov S, Ereameev A, Kholoptsev V, Plotnikov I,
718 Rybakov K, Semenov V, Sorokin A (2010) Effects of microwave
719 heating in nanostructured ceramic materials. *Powder Metallurgy
720 and Metal Ceramics*. 49:31–41

721 17. Chandrasekaran S, Basak T, Ramanathan S (2011) Experimental
722 and theoretical investigation on microwave melting of metals. *J
723 Mater Process Technol* 211:482–487

724 18. Srinath MS, Sharma AK, Kumar P (2011) A new approach to
725 joining of bulk copper using microwave energy. *Mater Des* 32:
726 2685–2694

727 19. Panda SS, Singh V, Upadhyaya A, Agrawal D (2006) Sintering
728 response of austenitic (316L) and ferritic (434L) stainless steel con-
729 solidated in conventional and microwave furnaces. *Scr Mater* 54:
730 2179–2183

731 20. Bose A, Agrawal D, Dowding RJ (2004) Preliminary investigations
732 into microwave processing of powder injection molded 17-4 PH
733 stainless steel. *International Conference on Powder Metallurgy and
734 Particulate Materials* 53

735 21. Quinard C, Song J, Barriere T, Gelin JC (2011) Elaboration of PIM
736 feedstocks with 316L fine stainless steel powders for the processing
737 of micro-components. *Powder Technol* 208:383–389

738 22. Mariappan R, Kumaran S, Rao TS (2009) Effect of sintering atmo-
739 sphere on structure and properties of austeno-ferritic stainless steels.
740 *Mater Sci Eng A* 517:328–333

Q3 741 23. Ertugrul O, Park H-S, Onel K, Willert-Porada M (2014) Effect of
742 particle size and heating rate in microwave sintering of 316L stain-
743 less steel. *Powder Technol* 253:703–709

744 24. Shi JJ, Cheng Z, Gelin JC, Barriere T, Liu B Multi-physic coupling
745 and full cycle simulation of microwave sintering, *The Advances in
746 Materials and Processing Technologies, AMPT 2015 Conference,*
807 December 14–17 2015, Madrid, Spain, In Symposium: New Trends
in Powder Metallurgy, 1–6 747
748

25. Shi JJ (2014) Experiment and simulation of micro-injection mold-
ing and microwave sintering, [Co-tutorial PhD Thesis]:
Chengdu&Besancon: Southwest Jiaotong University & Franche-
Comte University 749Q4
750
751
752

26. Song J, Gelin JC, Barriere T, Liu B (2006) Experiments and nu-
merical modelling of solid state sintering for 316L stainless steel
components. *J Mater Process Technol* 177:352–355 753
754
755

27. Yang RB, Liang WF, Lou CW, Lin JH (2012) Electromagnetic and
microwave absorption properties of magnetic stainless steel powder
in 2-18 GHz. *J Appl Phys* 111:07A338 756
757
758

28. Bahadoor A, Wang Y, Afsar MN (2005) Complex permittivity and
permeability of barium and strontium ferrite powders in X, KU, and
K-band frequency ranges. *J Appl Phys* 97:105–107 759
760
761

29. Kong X, Barriere T, Gelin JC (2012) Determination of critical and
optimal powder loadings for 316L fine stainless steel feedstocks for
micro-powder injection molding. *J Mater Process Technol* 212:
2173–2182 762
763
764
765

30. Quinard C, Barriere T, Gelin JC (2009) Development and property
identification of 316L stainless steel feedstock for PIM and μPIM.
Powder Technol 190:123–128 766
767
768

31. Enneti RK, Shivashankar TS, Park SJ, German RM, Atre SV
(2012) Master debinding curves for solvent extraction of binders
in powder injection molding. *Powder Technol* 228:14–17 769
770
771

32. Nayer A (1997) *The metals data book*. McGraw-Hill, New York
(NY) 772
773

33. Kim-Hak O, Soulier M, Szkutnik PD, Saunier S, Simon J, Goeuriot
D (2012) Microwave sintering and thermoelectric properties of p-
type (Bi_{0.2}Sb_{0.8})₂Te₃ powder. *Powder Technol* 226:231–234 774
775
776

34. Chen YC, You HM (2015) Effect of sintering temperature on mi-
crostructures and microwave dielectric properties of Zn₂SnO₄ ce-
ramics. *Mater Chem Phys* 154:94–99 777
778
779

35. Ma J, Diehl JF, Johnson EJ, Martin KR, Miskovsky NM, Smith CT,
Weisel GJ, Weiss BL, Zimmerman DT (2007) Systematic study of
microwave absorption, heating, and microstructure evolution of
porous copper powder metal compacts. *J Appl Phys* 101:074906 780
781
782
783

36. Yoshikawa N (2010) Fundamentals and applications of microwave
heating of metals. *The Journal of Microwave Power and
Electromagnetic Energy* 44:4–13 784
785
786

37. Seerane M, Ndlangamandla P, Machaka R (2016) The influence of
particle size distribution on the properties of metal injection-
moulded 17-4 PH stainless steel. *J of the Southern Africa Institute
of Mining and Metallurgy* 116:935–940 787
788
789
790

38. Gulsoy HO, Ozgun O, Bilketay S (2016) A powder injection mold-
ing of Stellite 6 powder: sintering, microstructural and mechanical
properties. *Mater Sci Eng A* 651:914–924 791
792
793

39. Gasko M, Rosenberg G (2011) Correlation between hardness and
tensile properties in ultra-high strength dual phase steels. *Mater Eng*
18:155–159 794Q5
795
796

40. Shen Y, Chawla N (2001) On the correlation between hardness and
tensile strength in particle reinforced metal matrix composites.
Mater Sci Eng A 297:44–47 797
798
799

41. MPIF (2007) *Materials standard for metal injection molded parts*,
MPIF standard 35. Metal Powder Industries Federation, Princeton
NJ, pp 19–19 800
801
802

42. Schönbauer BM, Yanase K, Endo M (2016) The influence of var-
ious types of small defects on the fatigue limit of precipitation-
hardened 17–4PH stainless steel, in press, *Theoretical and
Applied Fracture Mechanics* xxx xxx–xxx 803
804
805
806

AUTHOR QUERIES

AUTHOR PLEASE ANSWER ALL QUERIES.

- Q1. Please Glossary if presnted correctly.
- Q2. References has been sorted. Please check if correct.
- Q3. References 23 and 24 based on the original manuscript we received were identical. Hence, the latter was deleted and the reference list and citations were adjusted. Please check if appropriate.
- Q4. Please provide complete bibliographic details for references 25 and 38.
- Q5. Please check if the captured book title for reference 39 is correct.

UNCORRECTED PROOF